Journal of Applied Mechanics and Technical Physics, Vol. 38, No. 1, 1997

PRANDTL–MEYER EXPANSION OF A MIXTURE OF GASES WITH A LARGE DISPARITY IN MOLECULAR MASSES

S. V. Dolgushev and V. M. Fomin

UDC 533.6.011.8

Inhomogeneous flow of a gas mixture consisting of molecules with a large disparity in molecular masses involves the temperature and velocity differences of the components [1–3]. The comparatively small rates of momentum and energy exchange between molecules of various kinds lead to establishment of the Maxwellian velocity distribution inside each component individually and to the absence of the common temperature and mean velocity of the mixture as a whole. In this case, the flow of the mixture can be regarded as a combination of local-equilibrium flows of individual components interacting between each other through the relaxation of the temperatures and mean velocities of the molecules. This model was called the theory of a two-fluid medium [4–6]. It yields an adequate description of the temperature–velocity nonequilibrium and a number of phenomena typical of mixtures, for example, the change of mechanisms of ultrasound propagation [7], noncoincidence of the density and temperature profiles of the components in a strong shock wave [6], and rotational alignment of the linear molecules in supersonic jets and molecular beams [8]. The slip of the components leads to local changes in the medium's composition, which allows the use of this phenomenon for separation of gas mixtures and isotopes [1–3].

One of the types of motion of a gas with a strong inhomogeneity of the parameters is the Prandtl–Meyer expansion [9]. A sudden expansion of the gas near the corner point occurs with frozen physical and chemical processes at distances of the order of the relaxation length. Further evolution of the flow and establishment of equilibrium is determined by a system of equations of gas dynamics and kinetics.

In this paper, the flow of a helium–argon mixture with thermal and velocity nonequilibrium in a Prandtl–Meyer expansion fan and behind it near an inclined wall is studied numerically (using the method of characteristics and the conservative MacCormack scheme). We obtain the distributions of the flow parameters of individual components of the mixture with height above the surface of an inclined wall, which allow one to analyze the course of thermal and velocity relaxation and the changes in the mixture's composition, and also the qualitative pattern of separation of a small portion of the mixture into heavy and light components in flow about a corner point.

1. Formulation of the Problem. In Fig. 1, the ray OA which emanates from the corner point O is the fore front of a frozen helium-expansion fan which is ahead of the corresponding fronts of the equilibrium expansion fan of the mixture and of the frozen argon-expansion fan. An angle α_{01} is the Mach angle calculated from the frozen sound velocity of helium in a free stream ($\alpha_{01} = \arcsin \mathrm{M}_{01}^{-1}$, $\mathrm{M}_{01} = V_0/(\gamma R_1 T_0)^{1/2}$, M is the Mach number, V is the gas velocity, $\gamma = 5/3$ is the ratio of specific heats, R is a gas constant, and T is the temperature; the subscript 0 refers to the free-stream parameters, and the subscripts 1 and 2 indicate the parameters of the light and heavy components, respectively). The section of the ray OA is the upper boundary of the computational domain, and the section of the inclined wall OB is its lower boundary. Figure 1 does not show the forward and backward boundaries of the computational domain located, respectively, at small ($\sim 0.01\, l_{01}$, where l_{01} is the mean free path of helium molecules, which is calculated for free-stream conditions) and sufficiently large ($\sim 2000\, l_{01}$) distances downstream from the point O. The particular shape of these boundaries depends on the computation method used: for the method of characteristics, the boundaries are sections of the characteristics of the negative family of the light component, and for the MacCormack

Institute of Theoretical and Applied Mechanics, Siberian Division, Russian Academy of Sciences, Novosibirsk 630090. Translated from Prikladnaya Mekhanika i Tekhnicheskaya Fizika, Vol. 38, No. 1, pp. 65–70, January–February, 1997. Original article submitted August 9, 1995; revision submitted October 16, 1995.

 0021-8944/97/3801-0058 $18.00

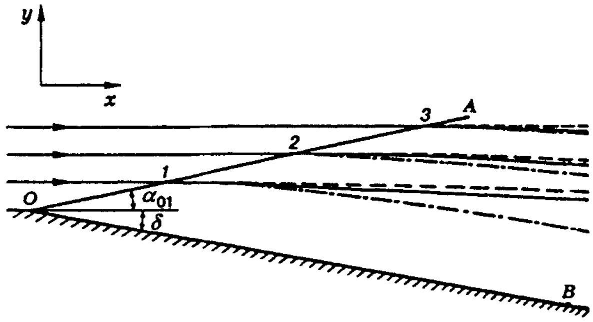

Fig. 1

scheme, they are lines perpendicular to the inclined wall. The free-stream parameters are specified as boundary conditions on the ray OA, the parameters of the frozen Prandtl–Meyer expansion of the mixture components are set for the forward boundary, and no boundary conditions are given for the backward boundary, since all characteristics appear there. The no-slip condition is specified on the wall OB, which in computation by the method of characteristics means the coincidence of the inclination angles of the components' velocities with the wall-inclination angle, and for the MacCormack scheme, it is approximated using the principle of reflection.

Computations were performed for the free-stream Mach number $M_0 = 7$ and 12, wall-inclination angle $\delta = 10°$, $p_0 = 10^{-2}$ N/m, and $T_0 = 100$ K. It turned out that for the model of a gas consisting of solid spheres, the results are not dependent on the concrete values of p_0 and T_0 if the flow is characterized by parameters normalized to the free-stream parameters, and spatial variables are measured in units of l_{01}.

2. Equations of Two-Fluid Gas Dynamics. Without considering viscosity and heat conduction, a steady planar motion of a gas mixture is governed by the system of equations of two-fluid gas dynamics in the Eulerian approximation [6]:

$$\frac{\partial \rho_i u_i}{\partial x} + \frac{\partial \rho_i v_i}{\partial y} = 0; \tag{2.1}$$

$$u_i \frac{\partial u_i}{\partial x} + v_i \frac{\partial u_i}{\partial y} + \frac{1}{\rho_i}\frac{\partial p_i}{\partial x} = -\frac{K}{\rho_i}(u_i - u_j); \tag{2.2}$$

$$u_i \frac{\partial v_i}{\partial x} + v_i \frac{\partial v_i}{\partial y} + \frac{1}{\rho_i}\frac{\partial p_i}{\partial y} = -\frac{K}{\rho_i}(v_i - v_j); \tag{2.3}$$

$$\frac{3}{2} n_i k \left(u_i \frac{\partial T_i}{\partial x} + v_i \frac{\partial T_i}{\partial y}\right) = -p_i \left(\frac{\partial u_i}{\partial x} + \frac{\partial v_i}{\partial y}\right) - q(T_i - T_j) + æ_{ij} K (\mathbf{U}_i - \mathbf{U}_j)^2; \tag{2.4}$$

$$n_i = p_i/(kT_i).$$

Here n, ρ, and p are the particle density, mass density, and pressure, $\mathbf{U}$ is the velocity vector which has components (u, v) in the Cartesian coordinate system (x, y), k is the Boltzmann constant, and the subscripts i and j take on the values 1 and 2. Using the formulas presented in [6, 10], we obtain

$$q = \frac{3R_1R_2}{R_1 + R_2} K, \qquad æ_{ij} = \frac{T_i/m_i}{T_1/m_1 + T_2/m_2}, \qquad K = \frac{p_1 p_2}{p_1 T_2 + p_2 T_1} \frac{T_{12}}{D_{12}(p, T_1, T_2)},$$

$$T_{12} = \frac{m_1 T_1 + m_2 T_2}{m_1 + m_2}, \quad D_{12}(p, T_1, T_2) = \frac{3k^2 T_1 T_2}{8p\sigma_{12}^2}\left(\frac{\pi}{2m_{12}kT_{12}}\right)^{1/2},$$

$$m_{12} = \frac{m_1 m_2}{m_1 + m_2}, \quad p = p_1 + p_2, \quad p_i = R_i \rho_i T_i,$$

where m is the mass of a molecule and $\sigma_{12} = 0.5(\sigma_1 + \sigma_2)$ is the effective collisional diameter of two different molecules ($\sigma_1 = 2.19 \cdot 10^{-10}$ m and $\sigma_2 = 3.66 \cdot 10^{-10}$ m).

3. Computations by the Method of Characteristics. If $M_i > 1$ for $i = 1$ and 2, the following characteristic relations are obtained from Eqs. (2.1)–(2.4):

$$\frac{dJ^+}{d\xi_i} = \frac{\cos\alpha_i}{\rho_i V_i^2}\Pi_i^+ - \frac{0.4\sin\alpha_i}{p_i V_i}\Phi_i; \tag{3.1}$$

$$\frac{dJ^-}{d\eta_i} = -\frac{\cos\alpha_i}{\rho_i V_i^2}\Pi_i^- + \frac{0.4\sin\alpha_i}{p_i V_i}\Phi_i; \tag{3.2}$$

$$\frac{dS_i}{d\sigma_i} = -\frac{2}{3}\frac{\Phi_i}{p_i V_i}; \tag{3.3}$$

$$\frac{dH_i}{d\sigma_i} = -\frac{\chi_i + \Phi_i}{\rho_i V_i^2}, \quad i = 1,\, 2. \tag{3.4}$$

In (3.1)–(3.4), we have $\alpha_i = \arcsin M_i^{-1}$, $H_i = h_i + 0.5\,V_i^2$, $h_i = (\gamma/(\gamma-1))p_i/\rho_i$, $V_i^2 = u_i^2 + v_i^2$, $S_i = \ln(p_i/\rho_i^\gamma)$, J_i^+ and J_i^- are determined by the differential relations $dJ_i^\pm = d\psi_i \pm (\mathrm{cotan}\alpha_i/\rho_i V_i^2)\,dp_i$ (ψ_i is the angle of inclination of the velocity vector of the ith component toward the free-stream direction), $\Phi_i = q(T_i - T_j) - æ_{ij}K[V_1^2 + V_2^2 - 2V_1V_2\cos(\psi_i - \psi_j)]$, $\Pi_i^\pm = K\{V_i\tan\alpha_i \mp V_j\cos(\psi_i - \psi_j)[\tan(\psi_i - \psi_j) \pm \tan\alpha_i]\}$, $\chi_i = KV_i[V_i - V_j\cos(\psi_i - \psi_j)]$, ξ_i, η_i, and σ_i are, respectively, the distances counted along the C_i^+, C_i^-, and C_i^0 characteristics of system (2.1)–(2.4) which have angles of inclination toward the x-axis equal to $\psi_i + \alpha_i$, $\psi_i - \alpha_i$, and ψ_i. In the free stream, with a moderate deviation from equilibrium, the Mach number of the heavy component is considerably larger than the corresponding Mach number of the light component at a given point of space due to a substantial difference in the frozen sound velocities of the components. If the directions of the velocity vectors $\mathbf{U}_1$ and $\mathbf{U}_2$ are slightly different, the streamline of helium and all characteristics of argon coming to a certain point of the plane $(x,\, y)$ are located between the C_1^+ and C_1^- characteristics of helium arriving at this point.

This configuration of the characteristics is shown in Fig. 2. The solution is assumed to be known on the curve AB, and the flow parameters should be calculated at the point C (the point C is the intersection of the helium Mach contours that emanate from the points A and B). Computations were mainly performed using the same scheme as in the usual method of characteristics for a one-fluid medium [11], and the search for the points of intersection with the curve AB and a subsequent interpolation of the parameters for this point are performed not only for the helium streamline, but for all characteristics of argon. To find the coordinates of the point C and to calculate the increments of J_1^+ and J_1^- on the sections AC and BC, we employed the same iteration method of successive approximations as in the commonly used method of characteristics [11]. Inside this iteration cycle, there was a Newtonian solution of a nonlinear system of characteristic difference equations that relate all other flow parameters at the point C to the known solution at points D, E, F, and G.

The layer-by-layer computations using the method of characteristics were performed, beginning with the C_1^+ characteristic of the frozen helium-expansion fan OA (see Fig. 1) and then passing to the other characteristics of this family. The step of the angular variable was $\Delta\varphi = 10^{-4}$ rad, and the step of the spatial variables was $\Delta\xi_1$ and $\Delta\eta_1 \sim 0.05\,l_{01}$, where $l_{01} = (2^{1/2}\pi n_0 \sigma_{12}^2)^{-1}$. The initial stage of computations was fairly effective: 1–2 iterations were required for convergence of computations at each point of the mesh. However, the code efficiency was reduced further on, since a large number of iterations were needed, and the computations were terminated. This is due to the fact that at a certain stage of computation the configuration shown in Fig. 2 is distorted because of a strong nonequilibrium of flow near the corner point.

In the course of computations, the evolution of the streamlines of individual components and the evolution of the mixture as a whole were traced by finding the isolines of the stream functions of the components and also the overall stream function of the mixture. The initial values of the stream functions were given on the initial-data curve OA (see Fig. 1) assuming that a gas particle moves as a whole until this curve.

The dashed curves in Fig. 1 show the argon streamlines, the dot-and-dashed curves indicate the

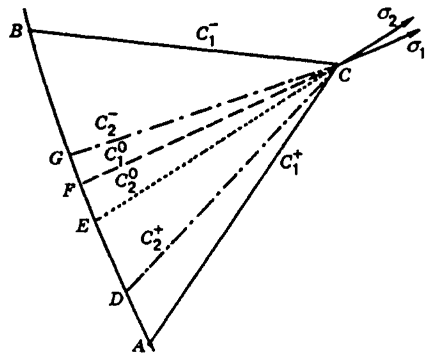

Fig. 2

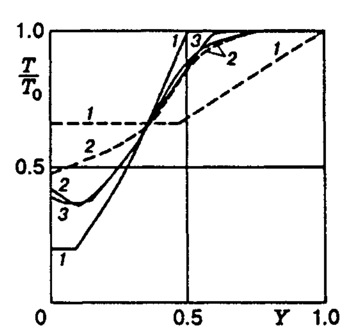

Fig. 3

helium streamlines, and the solid curves show the streamlines of the mixture as a whole (the latter are the trajectories of the centers of mass of the mixture's initially integral particles). The above-presented picture of decomposition of the mixture's particles was obtained for $\delta = 10°$, $M_0 = 7$, and the ratio of the molar concentrations of helium and argon was $c_1 : c_2 = 90:10$. The distances between the particles numbered 1–3 in Fig. 1 are l_{01}, $2\,l_{01}$, and $3\,l_{01}$ along the curve OA. Since the helium streamlines are more curved near the corner point O than the argon streamlines, the mixture is enriched in helium near the wall. The heavy-gas particles have a larger inertia, and their trajectories resemble the trajectories of the condensed-phase particles in two-phase flow past a convex corner. The effect of mixture separation is gradually attenuated with distance from the wall and disappears at large distances from the corner point at which the flow is in equilibrium.

4. Computations Using the Conservative MacCormack Scheme. If we choose the Cartesian coordinate system in a way such that the x axis is directed along the inclined section of the wall and then move over to the coordinates (X, Y) fitted to the surface in flow and determined by the relations $X = x$, $Y = y/(\tan\beta x)$, and $\beta = \alpha_{01} + |\delta|$, relations (2.1)–(2.4) can then be transformed into the following conservative form:

$$\frac{\partial \mathbf{E}}{\partial X} + \frac{\partial \mathbf{F}}{\partial Y} = \mathbf{G}. \tag{4.1}$$

Here $\mathbf{E} = X\tan\beta\mathbf{e}$, $\mathbf{F} = \mathbf{f} - Y\tan\beta\mathbf{e}$, $\mathbf{G} = X\tan\beta\mathbf{g}$, $\mathbf{e} = (\rho_1 u_1, \rho_1 u_1^2 + p_1, \rho_1 u_1 v_1, \rho_1 u_1 H_1, \rho_2 u_2, \rho_2 u_2^2 + p_2, \rho_2 u_2 v_2, \rho_2 u_2 H_2)^t$, $\mathbf{f} = (\rho_1 v_1, \rho_1 u_1 v_1, \rho_1 v_1^2 + p_1, \rho_1 v_1 H_1, \rho_2 v_2, \rho_2 u_2 v_2, \rho_2 v_2^2 + p_2, \rho_2 v_2 H_2)^t$, $\mathbf{g} = (0, Z, W, Q_1, 0, -Z, -W, Q_2)^t$, $Z = -K(u_1 - u_2)$, $W = -K(v_1 - v_2)$, and $Q_i = -q(T_i - T_j) + æ_{ij}K[(u_i - u_j)^2 + (v_i - v_j)^2] - K[u_i(u_i - u_j) + v_i(v_i - v_j)]$ $(i, j = 1, 2)$.

In the coordinate system (X, Y) in which the computational domain has a rectangular shape, the computations were performed using a semi-implicit MacCormack scheme [12], with the second-order approximation for both independent variables. The sequence of computations is commonly accepted for marching calculations of flow about corner configurations [13]. The section $0 \leqslant Y \leqslant 1$ was split into 100 equal parts, with $\Delta X \leqslant 0.4\Delta Y$.

Figures 3–5 show the results of computations for $\delta = 10°$, $M_0 = 7$, and $c_1 : c_2 = 50:50$. The temperature of the components normalized to the free-stream temperature is shown in Fig. 3 as a function of Y for various values of X. The dashed curves refer to helium, the solid curves refer to argon, and curves 1 correspond to the frozen expansion of two gases near the corner point ($X = 0.01\,l_{01}$). As X increases, the temperature of the components relaxes to a single equilibrium distribution. This is seen from the $T_1(Y)$ and $T_2(Y)$ plots for $X = 70\,l_{01}$ (curve 2) and $X = 500\,l_{01}$ (curves 3). With $X = 500\,l_{01}$, $T_1 \approx T_2$ for all values of Y. If the concentration of one of the components is small (~1%), the distribution of the temperature of the main component Y is practically not dependent on X (the self-similar Prandtl–Meyer distribution takes place everywhere, and the temperature distribution of the seeded component relaxes to it).

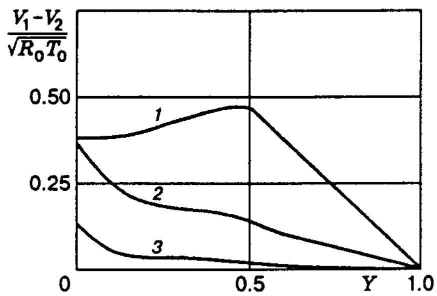

Fig. 4

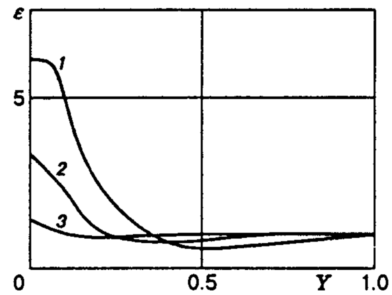

Fig. 5

The character of velocity relaxation of the components is given in Fig. 4, which shows the nondimensional velocity difference $(V_1 - V_2)/(R_0T_0)^{1/2}$ vs. Y (R_0 is a gas constant of the mixture in the free stream). Curve 1 corresponds to the frozen expansion near the corner point, curve 2 refers to $X = 7\,l_{01}$, and curve 3 refers to $X = 70\,l_{01}$ (the slip of the components practically vanishes in the larger part of the region of Y variation).

Figure 5 shows the coefficient of enrichment of the mixture in helium $\varepsilon = (n_1/n_2)/(n_1/n_2)_0$ vs. Y for various values of X. Curve 1 corresponds to the frozen flow near the corner point. The $\varepsilon(Y)$ plot becomes gently sloping with distance downstream from the point O along the wall OB, the maximum value of $\varepsilon\,(Y = 0)$ is substantially reduced, and $\varepsilon = 1$ in the main region of Y variation ($0.1 \leqslant Y \leqslant 1$). Curves 2 and 3 refer to the dependence $\varepsilon(Y)$ for $X = 70\,l_{01}$ and $1250\,l_{01}$. One can see that unlike the velocity and temperature relaxations, which are mainly completed at $X \sim (100\text{–}500)\,l_{01}$ from the corner point, the mixture near the wall ($Y \leqslant 0.1$) relaxes more slowly and, consequently, the mixture's composition near the wall is different from that in the free stream up to distances of $\sim(1500\text{–}2000)\,l_{01}$ from the point O. A gas layer with an increased content of helium is formed near the wall. The qualitative behavior of the coefficient of enrichment ε remains the same for various flow parameters and mixture composition. As the free-stream parameters δ and M_0 increase, the derivatives $\partial\varepsilon/\partial X$ and $\partial\varepsilon/\partial Y$ and the values of ε ($Y = 0$) increase as well.

5. Conclusions. The following conclusions can be drawn on the basis of the results obtained in the study presented.

(1) A layer of mixture is formed near an inclined wall, in which the process of velocity and temperature relaxation of the components propagates over large distances from the corner point. In essence, this corresponds to the concept of the existence of a near-wall entropy (vortex) layer in the Prandtl–Meyer flow with arbitrary-type nonequilibrium processes [14].

(2) The near-wall gas layer is substantially enriched in the light component. The coefficient of enrichment increases with increasing the free-stream Mach number and the angle of rotation of the wall at the corner point.

(3) The qualitative picture of divergence of the trajectories of the light and heavy components of a small portion of the mixture in the expansion fan is consistent with the inertial mechanism of separation of the mixture.

(4) A qualitative difference is seen between the process of velocity and temperature relaxation in the mixture with high molar concentrations of both components and that in the mixture with a seeded component. In the first case, the relaxation process is accompanied by considerable changes in the parameters of both components which lead to establishing a general equilibrium, while in the second case, the parameters of the seeded component relax to the parameters of the carrier components, which can be considered unaffected by relaxation and governed by the self-similar Prandtl–Meyer solution for a pure gas.

REFERENCES

1. V. H. Reis and J. B. Fenn, "Separation of gas mixtures in supersonic jets," *J. Chem. Phys.*, **39**, No. 12, 3240–3250 (1963).
2. R. J. Cattolica, R. J. Gallagher, J. B. Anderson, and L. Talbot, "Aerodynamic separation in free jet expansion," *AIAA J.*, **17**, No. 4, 344–355 (1979).
3. R. Compargue, J. B. Anderson, J. B. Fenn, et al., "Sur les methodes aerodynamique de separation dez gaz et isotopes," *Entropie*, **12**, No. 67, 11–33 (1976).
4. E. Goldman and L. Sirovich, "Equations for gas mixtures," *Phys. Fluids,* **10**, No. 9, 1928–1940 (1967).
5. C. J. Goebel, S. M. Harris, and E. A. Johnson, "Two-temperature disparate-mass gas mixtures: a thirteen moment description," *Phys. Fluids*, **19**, No. 5, 627–635 (1976).
6. S. P. Kiselev, G. A. Ruev, A. P. Trunev, et al., *Shock-Wave Processes in Two-Component and Two-Phase Media* [in Russian], Nauka, Novosibirsk (1992).
7. J. R. Bowler and E. A. Johnson, "Anomalous dispersion in disparate mass gas mixtures," *Phys. Rev. Lett.*, **54**, No. 4, 329–332 (1985).
8. S. DePaul, D. Pullman, and B. Friedrichs, "Pocket model of seeded supersonic beams," *J. Phys. Chem.*, **97**, No. 10, 2167–2171 (1993).
9. G. I. Abramovich, *Applied Gas Dynamics* [in Russian], Part 1, Nauka, Moscow (1991).
10. J. D. Ramshaw, "Hydrodynamic theory of multicomponent diffusion and thermal diffusion in multitemperature gas mixtures," *J. Non-Equil. Thermodyn.*, **19**, No. 2, 121–134 (1993).
11. O. N. Katskova and A. N. Kraiko, *Calculation of plane and axisymmetric supersonic flows with irreversible processes* [in Russian], Computing Center, USSR Acad. Sci., Moscow (1964).
12. R. J. LeVeque and H. C. Yee, "A study of numerical methods for hyperbolic conservation laws with stiff source terms," *J. Comput. Phys.*, **86**, No. 1, 187–210 (1990).
13. V. Shankar, D. Anderson, and P. Kutler, "Numerical solution for supersonic corner flow," *J. Comput. Phys.*, **17**, No. 2, 160–180 (1975).
14. V. P. Agafonov, V. K. Vertushkin, A. A. Gladkov, and O. Yu. Polyanskii, *Nonequilibrium Physical and Chemical Processes in Aerodynamics* [in Russian], Mashinostroenie, Moscow (1972).